Annu. Rev. Phys. Chem. 1999. 50:413–41

CONTROLLED MOLECULAR ADSORPTION ON SILICON: Laying a Foundation for Molecular Devices

Robert A. Wolkow
Steacie Institute for Molecular Sciences, National Research Council of Canada, 100 Sussex Drive, Ottawa, Ontario K1A 0R6, Canada; e-mail: bob.wolkow@nrc.ca

Key Words nanostructure, STM, silicon, molecular electronics, sensors

■ **Abstract** This review is about understanding and controlling organic molecular adsorption on silicon. The goal is to provide a microscopic picture of structure and bonding in covalently attached molecule-silicon surface systems. The bias here is that an unprecedented, detailed understanding of adsorbate-surface structures is required in order to gain the control necessary to incorporate organic function into existing technologies or, eventually, to make new molecule-scale devices. A discussion of recent studies of adsorbate structure is presented. This includes simple alkenes, polyenes, benzene, and carene adsorbed on Si(100). Also included is a discussion of wet chemical procedures for forming alkyl and alkoxy covalently functionalized silicon. These discussions are presented together with comments on the related issues of adsorption dynamics and nano-scale manipulation in an effort to point the way toward principles and procedures that will allow the hybrid properties of organic molecules and surfaces to be harnessed.

INTRODUCTION

This review is about understanding and controlling organic molecular adsorption on silicon. The goal is to provide a microscopic picture of structure and bonding in covalently attached molecule-silicon surface systems. The bias is that an unprecedented, detailed understanding of adsorbate-surface structures is required in order to gain the control needed to incorporate organic function into existing technologies or, eventually, to make new molecule-scale devices. A discussion of recent studies of adsorbate structure is presented together with comments on the related issues of adsorption dynamics and nano-scale manipulation in an effort to point the way toward principles and procedures that will allow the hybrid properties of organic molecules and surfaces to be harnessed.

Si(100) and unreconstructed Si(111) are, for the most part, the subject surfaces. A few results of broad impact that focus on other surfaces [Si(111)-(7 × 7) and

0066-426X/99/1001-0413$08.00

various metals] or on atomic adsorbates are also covered. The greater part of this review describes and discusses the organic molecule-silicon cases that are fully, or at least largely, understood. This section includes discussions of both dry and wet processes. "Dry" refers to dosing molecules onto a surface in a vacuum chamber. "Wet" processes are chemical modifications performed in solutions. Inclusion of the latter area, though unconventional, is important because entirely new possibilities are emerging from it.

The review proceeds by offering a motivation for work in the area of organic molecular adsorption on silicon. Next, a historical context for the work reviewed is provided, and the experimental and theoretical tools that have been most important in getting us to our present level of understanding are described. After the review of organic Si structures, issues related to adsorption dynamics are briefly discussed. The ways that a molecule tumbles and migrates and disposes of energy before coming to rest are challenging and important issues that place constraints on the control with which adsorbates may be configured. The next section touches on developments in nano-scale manipulation to provide hints of how we might (*a*) characterize organic-silicon systems in electrical terms, and (*b*) build simple prototypical devices.

Before proceeding, I wish to mention a few related areas that are not covered here. Whitesides has discussed the interesting properties and potential applications of self-assembled monolayers (1). [For a detailed structural analysis of these alkyl layers see Camillone et al (2).] There is enormous interest in devices made by means of organic metal insulator semiconductor field-effect transistor technologies and in organic light-emitting diodes. In these devices, function depends on properties of the amorphous molecular solid; precise control over molecular configuration and placement are not important (for examples see 3, and references therein). Built on a similar scale, organic based structures known as chemical sensor arrays (4) are generating much interest. With an interest more in line with the present discussion, Gimzewski and coworkers have studied large molecules—porphyrins and fullerenes on metals—with a focus on patterning and rudimentary device concepts (5). Structural determinations of small adsorbed molecules on metal surfaces continue to progress (6). Clusters have received much attention as interesting molecule-like entities (7). Progress has been made in modeling properties of surface-mounted clusters (8). The scanning tunneling microscope (STM) has been used to provide detailed characterization of small Fe clusters on GaAs (9) and silicon clusters on Si(111) (10), and a novel method for making and depositing clusters has recently been demonstrated (11).

MOTIVATION

The driving force behind efforts to marry organic molecules with silicon-based device technology is the expectation that this hybrid approach will enable the creation of new devices.

Although no one can foretell where successful applications will be found, it seems likely that organic molecules with their myriad and tunable properties, including size, shape, absorption spectrum, flexibility, chemical affinity, and conductivity, will create new functional possibilities. The idea promoted here is not to supplant silicon technology but to enhance it. We look toward functions for which silicon devices are not well suited: for example, light emission, light detection, and chemical sensing—all things that molecules can do very well. Admittedly, there are many steps between attaching a molecule to a surface and creating a functional hybrid device, but unquestionably, we have to begin with the first step.

About 20 years ago there was a burst of interest in what came to be called molecular electronics. This term was a catchall for many and varied schemes. The idea in general terms was to create assemblies of molecules to create complex functional units, for example, switches or transistors. Many ideas involving molecules on silicon were put forward; a good sampling can be found in the paper by Carter (12), one of the field's most active participants. Of course, drawing a molecular device and building one are very different things. Before the advent of the STM (13) there was no way to proceed. Indeed, until very recently there was not a single organic molecule-silicon surface system that was well understood. True molecular-scale devices remain far off but our collection of knowledge is growing rapidly. We are presently at the stage of understanding various options for molecular linkages to surfaces. It will soon be reasonable to begin asking detailed questions about the properties of small groups of molecules adsorbed on a silicon surface and how those hybrid characteristics might be harnessed.

HISTORICAL OVERVIEW AND ENABLING DEVELOPMENTS

Atomic-level study of Si(100) began in the 1950s with the landmark work of Schlier & Farnsworth (14). Over the following three decades the development of modern surface science and a detailed understanding of Si surfaces were closely coupled. Eventually, STM was used to provide a direct view of silicon dimers, ruling out nondimer-based models of the surface (15). The last substantial issue, the structure of the dimer itself, was at last settled when tunable temperature cryogenic STM was developed (16) and applied to show that silicon dimers are not symmetric species with their bond parallel to the surface plane, but rather are bistable, buckled entities with one atom of the pair higher than the other (17). The STM results were built on the formative work of many others. [For excellent reviews see Schluter (18) and Duke (19). Reviews focused on more recent, primarily STM, studies have been written by Becker & Wolkow (20) and by Kubby & Boland (21).]

The study of atom-resolved chemistry started when Wolkow & Avouris showed that reacted and unreacted sites on a silicon surface are clearly distinguishable

(22, 23). Those studies showed that adsorbates quench dangling bond states, causing the affected site to appear as a depression in STM images. This became the standard framework for discussing adsorbates on silicon.

Early in the development of STM, Tersoff & Hamann created the theoretical framework for understanding the atomic-level resolution images that the technique provides (24). They showed that the tunneling current is proportional to the local density of states of the surface at the position of the tip. Lang provided clear explanations (predictions) for the characteristic signatures of chemically different atomic adsorbates (25). He showed, for example, that sulfur, an electronegative element, can appear as a pronounced protrusion in (filled) occupied-state images but as a weak feature, possibly a depression, in (empty) unoccupied states (26). By contrast, Na, an electropositive element, was shown to appear as a protrusion in unoccupied states and as a relatively weak feature in occupied states. More recently, in a combined experimental and theoretical study, the group of Eigler worked with Lang to explain images of Xe atoms physisorbed on a metal (27). Because Xe-atoms make virtually no contribution to the state density at the Fermi level, at the time it was surprising that they appeared as pronounced STM features. The theory shows that even though an adsorbate-derived resonance (in this case the Xe 6s) lies far from the Fermi energy, it may make the dominant contribution to the STM image if it extends spatially farther than the bare-surface wave functions.

In the current context this is an important result. The explanation for the appearance of organic molecular adsorbates, which would seem to have no resonant contribution to tunneling, is similar.

For both the small adsorbates initially studied by Wolkow & Avouris (22, 23), and for the relatively large molecules discussed in this review, the quenching of dangling bonds causes a reduction in local state density, but for the larger molecules, this is more than compensated for by a through molecule component that is due to a mixing of Si-derived and molecule-based states.

Hallmark and co-workers have shown that STM images of organic molecules weakly adsorbed on Pt(111) could be adequately modeled with extended Hueckel theory and that closely related molecules could in some cases be distinguished (28). Bocquet & Sautet have used combined semiempirical structural methods and electron scattering techniques developed by Sautet & Joachim (29, 30) to reproduce all the salient STM features of, for example, CO (31) and benzene on Pt(32).

ORGANIC MOLECULE-SILICON STRUCTURE DETERMINATIONS

In this section, organic molecule-silicon systems that are fully, or at least largely, understood are critically discussed. As much as possible, key methods of analysis are described.

Dry Methods

Ethylene and Acetylene

Ethylene Ethylene, C_2H_4, was the first organic molecular adsorbate on Si(100) for which a structure was determined. This case is important because the adsorption structure of C_2H_4 is mimicked by many other alkenes. Although studies began in the late 1980s, about a decade passed before the structure was fully solved. The first study of alkene adsorption on Si(100) focused on propylene, C_3H_6, not ethylene (33). In that work it was found that, unlike the saturated molecules methane and propane, propylene reacts spontaneously with the surface. The initial investigations of ethylene measured vibrational spectra with electron energy loss spectroscopy (EELS) (34) and determined that the molecule attains a di-σ bonded arrangement. Subsequently, the thermal desorption of ethylene was studied and a barrier to desorption of 1.65 ± 0.07 eV was extracted. It was shown that essentially all ethylene molecules desorbed intact. It was also argued, incorrectly as it turned out, that the Si-dimer bond was broken on ethylene adsorption. Eventually, rigorous theoretical modeling studies (36, 37) confirmed the di-σ model and showed that the Si-dimer bond remains intact.

In 1992, STM was used to examine ethylene-Si(100) (38). The results clearly showed an adsorbate-derived feature, symmetrically placed about one dimer. An STM image is shown in Figure 1*b*. Uniquely, the STM results made clear the preference for adsorbates to avoid nearest-neighbor positions. This is a preference, not a rule, because adsorbates do populate adjacent sites increasingly at higher coverage.

It is appropriate to insert some background regarding the Si dimer at this point. The silicon dimer displays properties intermediate between those of a double-bonded entity and a bi-radical. The clean Si dimer is σ-bonded with a small π-bonding contribution. Less-than-optimal π-bonding occurs because the Si dangling bonds are not parallel (the ideal arrangement) and therefore cannot interact

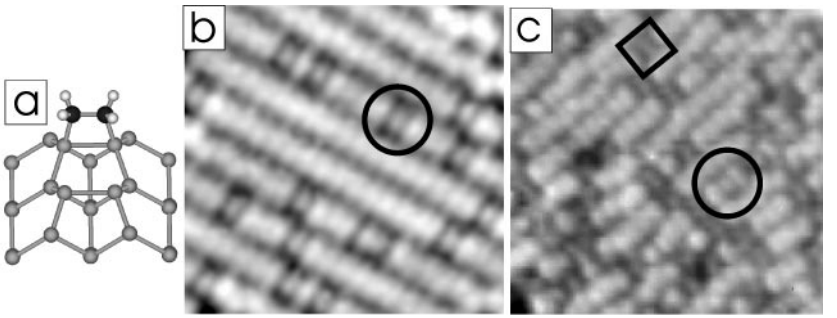

Figure 1 (*a*) Model of adsorbed ethylene on Si(100) in the di-σ configuration. (*b*) Occupied-state STM image of ethylene on Si(100) (93a). (*Open circle*) One adsorbate. (*c*) Occupied-state image of acetylene on Si(100) (from Reference 47). (*Open square*) A bridge-bound molecule; (*circle*) a one-dimer bound molecule.

strongly. Furthermore, silicon dimers are bistable, buckled units (17, and references therein). One Si-atom moves up (away from the surface) while the other moves down. The paired atoms are nonequivalent and therefore share an interaction similar to a heteronuclear bond. The up-atom becomes more nearly sp^3 in character and therefore a little lower in energy and more fully occupied. The down-atom becomes sp^2-like and has proportionately less local occupied-state density. The degree of π-bonding varies as the dimer fluctuates. The π interaction is optimal when, transiently, the dimer is symmetric (both atoms are of the same height). When the dimer is buckled, as it most often is, the dangling bonds are no longer degenerate and π-bonding is further disfavored. Finally on this point, it is incorrect to think of the splitting of the dimer surface state as due to a π-π^* interaction. The buckled dimer has associated with it an occupied-unoccupied pair of states. At the surface these form the valence- and conduction-band edges. This splitting, that is, this energy-lowering mechanism, is greater than a π-π^* interaction. This is why dimers are buckled and not symmetric.

For ethylene-Si(100), the symmetric structure of the adsorbate is shown in Figure 1*a*. The C-C bond adds across, and becomes parallel to, a Si dimer. Only this adsorption geometry is observed; the molecule is not observed to bridge dimers in a row or in adjacent rows. Calculated bond lengths are quoted from Pan et al (36): The Si-Si dimer bond lengthens from 2.26 Å to 2.33 Å—the dimer clearly remains intact. The C-C double bond, originally 1.34 Å in length, is reduced to a single bond of 1.52 Å. The C-atoms rehybridize from sp^2 to sp^3 as they become four-coordinate, forming σ-bonds with the Si dimer dangling bonds. The Si-C bonds are calculated to be 1.93 Å, in correspondence with the 1.89 Å bond length known for SiC. It is evident that this structure is strained; the C-atoms cannot attain a preferred sp^3 configuration and the Si dimer would ideally have outward-directed bonds. This mismatch is somewhat alleviated by accessible Si 3*d* levels that make varied bonding configurations accessible for Si.

Fisher and coworkers have shown that a simple STM simulation does a remarkably good job of describing ethylene-Si(100) (39, 40). There, constant-charge density contours predict the molecule to appear slightly higher than do clean dimers. Only when more detailed simulations including the effects of the electric field were performed were the dimers found to appear a little higher than the adsorbate, in accordance with experiment. It emerged that the electron density associated with the clean dimer dangling bonds is more polarizable than that in the vicinity of the molecule. This detailed understanding of image contrast may prove useful in the future. As a practical point, it is worth simply noting that an adsorbate about 2 Å above the Si(100) surface appears about as high in STM contours as the clean dimers.

Acetylene Acetylene was first studied by Nishijima et al (41), who used EELS, low-energy electron diffraction (LEED), and thermal desorption techniques to arrive at a di-σ bonded model of the adsorption geometry, a structure analogous to that assigned to adsorbed ethylene. In that work it was shown that acetylene

remained intact below room temperature, but that at elevated temperatures Si-H stretching was clearly visible, indicating that the molecule had decomposed. Preadsorption of atomic hydrogen on Si(100) was shown to saturate the silicon dangling bonds and block acetylene adsorption. Taylor et al subsequently studied the adsorption and decomposition of acetylene on Si(100) (42). There, a somewhat refined, but essentially unchanged, view of the thermal decomposition of adsorbed acetylene was stated. In that work, a di-σ bonded model was again concluded. It was also argued, as it had been for ethylene, that the affected Si-dimer bond was cleaved on formation of the complex (42). That view was challenged (43, 44) and eventually firmly overturned by theoretical modeling (37, 45). In 1992, EELS was again applied to acetylene-Si(100) (46). A key feature, not observed in the previous work, was the C-C stretch at 1450 cm^{-1}. Because this feature was very similar to that observed for silylethylene compounds (Si_2-C=C-Si_2), it was determined that a C-C double bond existed and that therefore the C-atoms were sp^2 hybridized. It was also pointed out that the $\sim$3000 cm^{-1} C-H stretch thought by Nishijima et al to be too low for an sp^2 C was actually as expected for an sp^2 C-atom bound to silicon.

This picture of acetylene adsorption, while appealing, is only part of the story. Recent STM measurements (47) are offered as confirmation of the di-σ configuration, but careful examination of the published images shows that (at least) two configurations are present (Figure 1*c*). At low coverage, the predominant structure of adsorbed acetylene clearly has a two-dimer footprint (see *square outline* in Figure 1*c*) and must therefore be due to a bridging structure involving two dimers. Some relatively rare single-dimer structures also appear to be present (*circled region*, Figure 1*c*). Early calculations indicated a stable bridge structure involving adjacent dimers in the same row where the molecule attached to one atom of each dimer (48). That particular bridge structure seems to be stable, as indicated by the symmetrical appearance of the observed structures. More recent calculations indicate two symmetric bridge structures for adsorbed acetylene (48a; also simulated images agree well with experiment). Each involves four Si-C bonds and reduction of the triple C-C bond to a single bond. Given the evidence of a dominant bridge structure, it is strange that the single-dimer structure is the calculated global minimum. At this point we can only speculate that the bridge structure, although more weakly bound, is more accessible kinetically to incoming molecules. Furthermore, since the bridge is stable at room temperature, it can be concluded that the bridge must be separated from the single-dimer structure by a barrier greater than $\sim$0.9 eV. At higher coverage, it was concluded that the one-dimer structure occupies every other dimer (47). In view of the above discussion, an alternate explanation is attractive: that the surface shown is dominated by the bridge structure.

Simple Alkenes

Propylene Propylene (CH_3-CH=CH_2) adsorption proceeds, not surprisingly, much like ethylene adsorption (33, 49). The molecule becomes alkane-like as two Si-C bonds are formed. Unlike ethylene, which appears as a slight depression

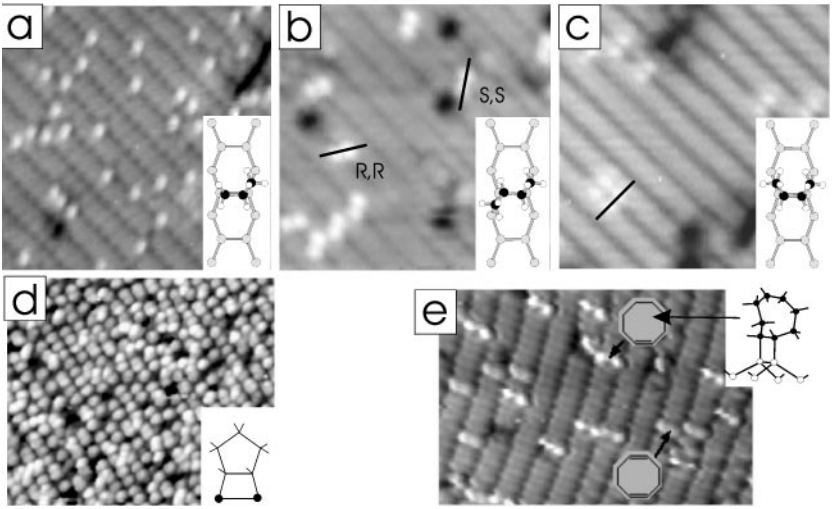

Figure 2 (*a*) Unoccupied-state STM image of propylene on Si(100) (from Reference 49). (*Inset*) Plan view of adsorbed propylene on a three-dimer portion of a Si(100) surface. (*b*) Unoccupied-state STM image of *trans*-2-butene on Si(100) (from Reference 49). (*Inset*) Plan view of the adsorbed molecule. (*c*) Unoccupied-state STM image of *trans*-2-butene on Si(100) (from Reference 49). (*Inset*) Plan view of the adsorbed molecule. (*d*) Occupied-state STM image of cyclopentene on Si(100) (from Reference 52). (*e*) Occupied-state STM image of cyclooctene and 1,5-cyclooctadiene on Si(100) (from Reference 52). (*Inset*) The upright configuration of cyclooctene.

in STM images, propylene displays a circular protrusion, about 0.5 Å above the dimers (see Figure 2*a*). The protrusion, which is off to one end of the attached dimer, is associated with the methyl group. It may seem somewhat surprising that the methyl group, which has no localized states resonant with the tunneling process, should appear as a protrusion. But tunneling can be significantly assisted by the mixing and broadening of adsorbate-derived states and we will see that this is the case for all organic adsorbates on Si(100). Effectively, silicon states decay less rapidly through the molecule than through vacuum, resulting in a protrusion positioned at, and with electronic characteristics of, the adsorbate.

Propylene-Si(100) displays an additional interesting feature not seen with ethylene. The methyl group protrudes off to one side, that is, it is nearer to one neighboring dimer than to the other. It is apparent that two types of adsorbed propylene must exist. These structures cannot be superimposed by a simple translation and a 180° rotation. In other words, the central carbon in the molecule becomes chiral on adsorption. Although not readily apparent from inspection of the image, it has been determined, by use of a lattice-matched grid overlay, that methyl protrusions in a dimer row are separated either by an integral number of dimer spaces or by that distance plus or minus two times the offset distance of the methyl from the dimer

bond. We see with propylene-Si(100) that the concept of chirality, an important theme in biochemistry, carries over to the surface realm (49). Issues of chirality and stereochemistry arise again in the following discussion of the 2-butenes, and again in the section on carene adsorption.

Cis- ***and*** **trans-*2-butene*** The chemical and physical properties of future hybrid organic molecule-microelectronic devices will depend on molecular structure and conformation. Molecular-recognition events, particularly chiral recognition, will be dependent on the stereochemistry of the adsorbed molecules. Lopinski et al have examined the utility of STM in monitoring and identifying geometric configurations on a molecule-by-molecule basis (49). Figures 2*b* and 2*c* show, respectively, STM images of *trans*-2-butene and *cis*-2-butene on Si(100). As discussed above for propylene, the protrusions are associated with the methyl groups. It is immediately apparent that the images of *cis*- and *trans*-2-butene are different. The methyl groups of the *cis* isomer define a line that is at a right angle to the dimer rows. By contrast, the *trans* isomer shows protrusions that define a line angled approximately 30° to the dimer row. In an earlier study of macroscopic samples, Kiskinova & Yates had shown that *cis*- and *trans*-2-butene exhibit different desorption energies from Si(100), demonstrating that the isomers retain their configuration on adsorption (50). In future studies of the formation and function of nanostructured patterns of molecules, extraordinary tools capable of probing subtle structural details will be required. The 2-butenes study has shown that STM is uniquely important in this regard.

Assignment of the bright protrusions to methyl groups was further justified by AM-1 calculations (49), as illustrated by the insets in Figure 2. The positions of the methyl groups in the images were found to be in quantitative agreement with the calculated bonding geometries. When the methyl protrusions of adsorbed molecules were registered with the underlying Si dimers, the methyl groups were displaced by approximately 1.1 Å from the center of those units. The distance between the paired protrusions of the *trans*-2-butene was measured to be 3.4 ± 0.2 Å, as compared with 3.6 Å obtained from calculation. More rigorous density-functional calculations gave very similar configurations and showed that the AM-1 method, cheaper by roughly 1000 times, can serve as a useful guide.

As illustrated by the 2-butene study, there is an additional and unique benefit to direct observation of the geometric isomers of single adsorbed molecules. Knowledge of the spatial relationship between methyl groups of a single reacted alkene provides an opportunity to determine the absolute configuration (*R* or *S*) for each newly formed asymmetric (chiral) center. An unsaturated bond such as that in *trans*-2-butene has two reactive faces that are associated with two distinct products. These are called the *Re* and the *Si* faces; the *Re* face leads to a product with *R* chirality (pro-*R*) and the *Si* face leads to a product with *S* chirality (pro-*S*). Thus the reaction of *trans*-2-butene leads to two chiral products (either to *RR* or to *SS*), whereas the reaction of *cis*-2-butene results in a nonchiral product (*RS* or *SR*). Because the *Re* and *Si* faces of *trans*-2-butene react with equal probability, an

equal number of *RR* and *SS* enantiomers are formed. Nevertheless, it is clear from Figure 2*b* that *RR* is distinguishable from *SS*. Similarly, by registering the methyl groups with the underlying lattice, the chirality of adsorbed *cis*-2-butene (*RS* or *SR*) was determined and provided the first direct determination of the absolute chirality of individual adsorbed molecules (49).

Those interested in stereochemistry at surfaces may wish to read an interesting recent paper describing the determination of chirality of large organic molecules adsorbed on graphite (51). Also, a later section in this paper describes carene, an alkene with one reaction face effectively blocked from surface reaction, which has been used to achieve asymmetric induction on Si(100).

Cyclopentene Hamers et al have studied cyclopentene with STM and infrared (IR) spectroscopy (52). Their analysis has shown that this molecule displays the expected ethylene-like adsorption behavior. The emphasis of the work was on forming an ordered organic monolayer by having the adsorbate follow the existing substrate crystallography. This was largely achieved. The majority of dimers have one molecule attached and those adsorbates are attached in a uniform manner, as depicted in Figure 2*d*.

Because the focus here is on details of adsorbate structure and interrelationships, it is interesting to take a closer look at the cyclopentene images. We see that subtle structural variations occur, roughly speaking, at about every fifth dimer. Typically, these appear as a smaller- or a larger-than-average gap between adjacent adsorbates or, on occasion, as a feature centered between dimer rows. The concentration of preexisting defects was not stated. (These typically exist at a level of a few percent). Perhaps the preexisting defects are a factor in the observed disruptions in order. The features between rows are likely impurities because other simple alkenes do not bridge rows.

The previously discussed propylene and 2-butene results showed that interesting structural options arise when the alkene carbon atoms are transformed to sp^3 species. For cyclopentene, it is expected that there should be a discernible lean to the molecule. This effect was not discussed in Hamers et al (52), but it is notable that the variable spacing described above is consistent with the molecules leaning one way or the other. It is a significant effect. The difference in spacing expected between two adsorbates leaning toward or away is several Angstroms. To go a step further, the observation that more often than not adsorbate spacing is uniform suggests that incoming adsorbates take note of the sense in which preexisting adjacent molecules are attached.

Cyclooctene Although cyclooctene adsorption on Si(100) has not been extensively studied, its structure appears to be straightforward. As with ethylene and other alkenes, cyclooctene attaches in the di-σ mode to one silicon dimer. In STM images, each adsorbed molecule shows two protrusions (53). These lie on a line directly above the attached dimer and are separated by approximately 5 Å (Figure 2*e*). STM images of cyclooctene are reported to often appear as indistinct

streaks. That behavior has been associated with the considerable height and floppiness of the adsorbed molecule.

Poly-enes

1,5-Cyclooctadiene The molecule 1,5-cyclooctadiene has been studied with STM, IR, and X-ray photoelectron spectroscopies, and by ab initio computation (54). STM images revealed that at high coverage ordered films of the molecule were formed. The degree of order achieved was not quantified. Through inspection of the published images, it is evident that the overlayer is roughly 5% disordered. It is possible that order is primarily limited by preexisting defects on the starting Si(100) surface. The defect density was not stated, but inspection of the reported low coverage image shows it to be ∼5%.

Determination that the molecule stands up, that is, it bonds through only one of its two C double bonds, was based on two observations. X-ray photoelectron spectroscopy C(1*s*) spectra were deconvoluted to reveal three chemically shifted peaks at 283.7, 284.4, and 284.8 eV, with relative intensities of a 1:2:1 ratio. These were interpreted as due to two C-atoms per molecule bonded to Si, four sp^3 carbons, and two sp^2 carbon atoms. The second observation pointing to an upright, single dimer-bound structure was an IR measurement that showed measurable alkene C-H stretching near 3020 cm^{-1}. A bridged structure would retain no alkene function and would show only alkane-type C-H stretching below 3000 cm^{-1}.

Although this substantial evidence does indeed point to the single dimer-bound structure, it is curious that the bridged structure does not form. An AM-1 calculation predicts that the bridge structure is substantially more stable with an adsorption energy of 2.5 eV compared with 1.2 eV for the one-dimer attached structure. This calculation method provides a very good guide because it agrees within 20% with ab initio (density functional theory B3LYP/6-31G*) adsorption energies for ethylene, *cis*-, and *trans* 2-butene and benzene adsorbates on Si(100). Rigorous ab initio calculation methods were employed to investigate 1,5-cyclooctadiene-Si(100) adsorption, but unfortunately, the model employed contained only one silicon dimer (54). It was pointed out that strain interferes with formation of the second alkene-dimer bonding interaction—a valid point—but the question remains: How big a barrier does this present? It was also noted that the molecule does not fit well in a bridged two-dimer position. Although this seems at first to be a compelling point, it turns out that great flexibility of molecule and surface are possible. The far poorer-fitting benzene molecule achieves a bridge structure (62–64); this is further discussed below.

The line section extracted from the low-coverage sample described in Padowitz & Hamers (53) shows that adsorbed 1,5-cyclooctadiene gives rise to a 1.2 Å protrusion. Cyclooctene (one double bond) gives rise to a much larger (not quantified) protrusion than does 1,5-cyclooctadiene (53). Figure 2*e* shows these two molecules coadsorbed. It also shows that the cyclooctene molecule adsorbs at a single dimer, whereas the 1,5-cyclooctadiene adsorbate clearly has a two-dimer footprint and gives rise to a protrusion centered between the affected dimers. If

the 1,5-cyclooctadiene molecule was standing up, leaving the alkene function protruding into the vacuum, it is expected that geometric and electronic effects would cause it to look at least as bright (as high) as the cyclooctene adsorbate—but that is not observed. The STM observations seem to better support the bridge than the unbridged structure.

This conflict between STM and IR data might be related to the nature of the 4° miscut single-domain silicon surface used for IR measurements. A significant fraction of that surface, on the order of 20% (in the vicinity of the double steps), is not a dimer reconstructed surface but a rebonded region of very different structure and character. Perhaps the observed alkene C-H stretch arises from anomalous (unbridged) adsorbates in the double-step region. IR spectra of normal single-stepped 1,5-octadiene-Si(100) are required to answer this question. Also, simple desorption measurements might distinguish between a single and a stronger bound bridge structure.

1,3-Butadiene and 1,3-Cyclohexadiene 1,3-Butadiene (CH_2=CH-CH=CH_2) and 1,3-cyclohexadiene are related molecules: Each has two alkene units separated by a single C-C bond. Conjugated dienes such as these can react with another alkene by Diels-Alder cycloaddition. There, carbon atoms 1 and 4 of the diene form new σ bonds to the C-atoms of the simple alkene to form a six-membered ring. C-atoms 2 and 3 of the diene become double-bonded and the simple alkene becomes single-bonded. Theoretical studies by Konecny & Doren have probed the possibility that a similar process involving a silicon dimer rather than a simple alkene might take place (55). An adsorption energy of 2.3 eV was determined for the Diels-Alder reaction of 1,3-cyclohexadiene with Si(100) when using density functional theory methods (B3LYP/6-31G**). The simple alkene addition (using only one of the two available double bonds) was also calculated and found to have an adsorption energy of 1.7 eV. Because the barrier controlling conversion of the simple alkene-addition product to the Diels-Alder product was, in any case, found to be negligible, it was predicted that the Diels-Alder product would be formed. Structures and vibrational spectra were calculated for 1,3-butadiene and for 2,3-dimethyl-1,3-butadiene as well. IR spectra were measured and found to be in agreement with the calculated spectra of the Diels-Alder products (56).

STM analysis of the 1,3-cyclohexadiene-Si(100) reaction has also been performed (57) (Figure 3*a*). Three distinct structures were observed. One thought to be the Diels-Alder product was labeled *X*. This structure looks very much like the image of one-dimer-bound benzene, as discussed further in the section that refers to benzene adsorption. The other two structures reported in Reference 57 were thought to be the results of single alkene addition. Alternate explanations for these two structures are offered in the discussion on benzene.

1,3,5,7-Cyclooctatetraene 1,3,5,7-Cyclooctatetraene appears to always bond through two of its alkene functions, most often in a symmetric fashion, to two adjacent dimers in the same row (58). It was noted that with two of the original four

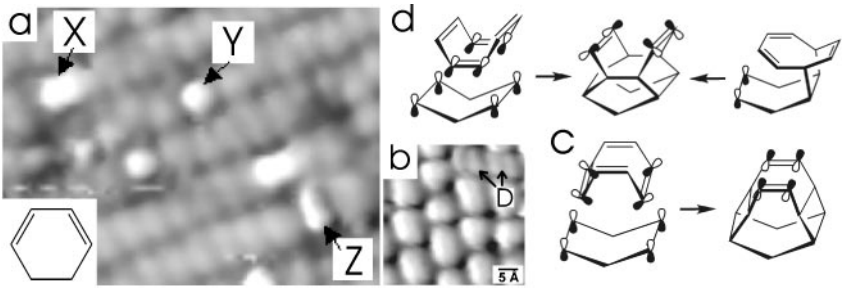

Figure 3 (*a*) Occupied-state STM image of 1,3-cyclohexadiene on Si(100) (from Reference 57). (*b*) Occupied-state STM image of 1,3,5,7-cyclooctatetraene on Si(100) (from Reference 58). (*c*) Schematic view of the reaction of 1,3,5,7-cyclooctatetraene at the Si(100) surface to create the double di-σ configuration. (*d*) Schematic view of two different reaction paths for 1,3,5,7-cyclooctatetraene at the Si(100) surface to create the tight-bridge or double Diels-Alder product.

alkene units remaining per adsorbed molecule, films of 1,3,5,7-cyclooctatetraene on Si(100) might have unusual electronic or optical properties (58).

The typical adsorbate configuration covers two dimers and appears as a protrusion slightly elongated along the dimer row direction (Figure 3*b*). These protrusions rise approximately 1.6 Å (at -2.0 *V* sample bias and 200 pA) relative to clean dimers. It was reported that, on examination of cross-sectional scans in the dimer row direction, a small dip on the order of 0.1 Å is intermittently evident in the protrusion (58).

1,3,5,7-Cyclooctatetraene was examined with the objective of forming highly ordered films and a high degree of order is apparent. A look at the details of the adsorbate shapes in the high coverage regime shows that approximately 10% of the molecules appear different from the typical adsorbate. The authors focus on one particular minority configuration, marked *D* in Figure 3*b*, that occurs at the level of about 5% (58). Relative to the most common configuration, this structure is less high and less elongated along the dimer row but wider in the dimer bond direction. This structure shows two parallel bar-like structures aligned with the dimer row. The structure of this species was not identified.

Two bridging structures were considered as candidates for the dominant configuration and were explored computationally. One configuration is a double di-σ structure that leaves two parallel alkene units aligned with the dimer row (Figure 3*c*). The other might be described as a tight bridge structure in analogy to the benzene bridge (see below) or, alternately, could be called a double Diels-Alder structure. This configuration leaves two parallel alkene functions aligned in the dimer bond direction (Figure 3*d*). The di-σ structure was optimized at the B3LYP/3-21+G* level. A calculated adsorption energy of 4.52 eV was found. Unfortunately, optimization of the tight bridge structure failed to converge, but it was noted that intermediate structures were less stable than the di-σ structure.

As a result, the di-σ structure was identified as the probable structure of the most common configuration seen.

Whereas we tend to expect the thermodynamic minimum to dominate, it is notable that, although less strongly bound, the tight bridge structure can account for elongation in the row direction and the weak minimum (sometimes seen) that runs across the molecule in the dimer bond direction. The di-σ structure seems an attractive candidate for the 5% minority structure, as it can account for the minimum running along the row and the two bar-like protrusions. Note that there is similarity in the appearance of 1,5-cyclooctadiene and the 5% minority cyclooctatetraene species: It is suggested here that both adopt a di-σ bridge structure.

Mechanistically, the possible existence of the tight bridge structure raises interesting questions. Two reaction paths are shown in Figure 3(*d*). The molecule could approach the surface with two C-double bonds aligned to bridge both ends of adjacent dimers, or alternately, the structure could form as a result of two Diels-Alder reactions. The double Diels-Alder scheme seems more reasonable. If that is the mechanism, a lower-temperature unbridged species may be isolable.

Examination of the published images also shows occasional (at the $\sim$1% level) bridging structures as well as somewhat more numerous relatively contracted structures. Insufficient data are available to speculate on the structure of these species. It can be said in conclusion that this molecule, which might be expected to display a relatively rich variety of adsorption geometries, does in fact do so.

Pentacene Pentacene adsorption on Si(100) has been studied with STM and AM-1 semiempirical molecular orbital computation by the Kawai group (59). The STM images of pentacene show that the molecule can adopt a number of configurations, aligned along the dimer row, crossing dimer rows at a right angle and crossing two rows at angles other than 90°. Details of registry with the lattice are not yet clear.

Beyond Alkenes

Benzene Benzene (C_6H_6) adsorption on Si(100) is the most complex molecular adsorption system yet solved. The tight bridge configuration that emerges as the ground state for benzene-Si(100) is a surprise because it involves a seemingly poor fit and the formation of a strained structure in which the substrate warps significantly in order to accommodate the adsorbate.

Recently, several groups simultaneously initiated study of benzene-Si(100). Borovsky et al used STM to find a metastable one dimer–bound structure that converted to a more stable structure of asymmetric appearance (60). The interpretation offered was in terms of the existing theory (61). The group of Wolkow (see References 62–64) used STM and found the same metastable and final state structures and, in addition, found a bridging species related to surface defects. The latter group also used IR spectroscopy and ab initio computational methods to show that the previous theoretical work was in part incorrect, and to identify the benzene adsorption structures. The computational work introduced a new inexpensive and

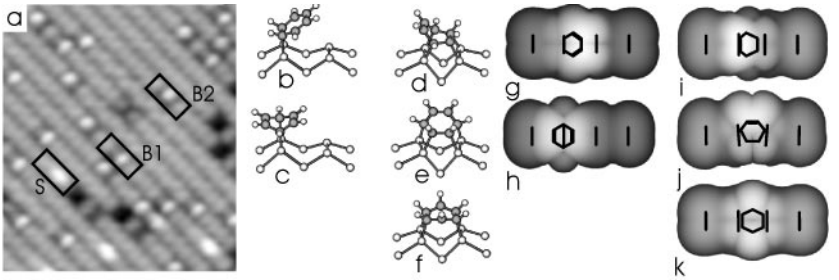

Figure 4 (*a*) STM image of benzene on Si(100) at 293°K ($V_{\text{sample}} = -1.5$ V, I = 40 pA). The labels indicate examples of single-dimer bound benzene (*S*) and two different bridging configurations (*B1* and *B2*). (*Rectangles*) The four-dimer units corresponding to the simulated images (*g*) through (*k*). (*b–f*) Schematic diagrams of benzene-Si(100) adsorption geometries. (*g–k*) Calculated charge density iso-surfaces of occupied valence states for the different bonding geometries considered. The Si-Si dimer bonds and the C-C bonds are indicated.

effective method for synthesizing STM images of calculated structures, thereby allowing candidate structures to be scrutinized with respect to adsorption energy and STM appearance. Use of detailed experimental and theoretical photoelectron spectroscopy analyses led to findings only of an unstable bridging structure and to the conclusion that no bridging structure existed, and as a result, to the incorrect identification of the ground state (65, 66).

As seen in the STM image in Figure 4*a*, room-temperature adsorption of benzene on Si(100) results in three distinct room-temperature–stable bonding configurations. The largest protrusions, labeled *S*, are centered over one dimer. The features labeled *B1* and *B2* occupy two dimers and are associated with bridge-bonded benzene. *B1* and *B2* are asymmetric with respect to the dimer row and the dimer bond, respectively. Although the single-dimer state, type *S*, is populated preferentially on adsorption, that state is observed to be metastable with respect to bridging configuration *B1*. Time sequences of images revealed that conversion of the single-dimer state to bridged state *B1* occurs with a time constant of $(1.50 \pm 0.05) \times 10^3$ *s*, which translates to an activation barrier of 0.94 eV (assuming a pre-exponential of 10^{13} s^{-1}) (62). A similar value, approximately 1 eV, was reported by Borovsky et al (60). Monitoring of the decay of the single-dimer state and the concomitant formation of the bridge state reveals that in forming a bridge bond, the molecule retains an interaction with the original adsorption site.

Two single-dimer bonding configurations must be considered for benzene, and are illustrated in Figures 4*b* and *c* (63, 64). The 1,2 configuration (denoting C-atoms 1,2) of Figure 4*b* is attractive because it is most analogous to adsorbed ethylene. Unlike ethylene, however, which has an adsorption energy on the order of 2 eV, the calculated (Hartree Fock 3-21G* optimization and single-point B3LYP/6-31G* energies, terminating H-atoms fixed in place) adsorption energy is

0.38 eV. This small value indicates that this species, if formed, would not remain adsorbed long enough to be imaged at room temperature. (Note the AM-1 method gives similar geometries for all five structures, the energies, however, are well off for the 1,2 and symmetric bridge (for details, see 64). In the 1,4 single-dimer geometry (Figure 4*c*), the molecule is bound through the most widely separated carbon atoms. The calculated adsorption energy is 1.04 eV. Experimental monitoring of desorption of the one-dimer species allows an adsorption energy of 1.05 eV (assuming a preexponential of 10^{13}) to be estimated (62). This agreement strongly indicates that the 1,4 species is the single-dimer species labeled *S* in Figure 4*a*. This species was also identified elsewhere (60, 61).

The 1,2 and the 1,4 one-dimer structures have much in common. The two carbon atoms directly involved in bonds to silicon become sp^3 hybridized, whereas the remaining four carbon atoms retain an sp^2 character. It is important to understand why the edge-bound benzene does not adsorb with a strength of interaction similar to that of ethylene. There are two factors at play. The extra stability of an aromatic molecule such as benzene is lost on chemisorption—this applies for the 1,2 and the 1,4 configuration. So whereas for ethylene adsorption the thermodynamics are dictated by the loss of a C-C π-bond and the gain of two Si-C bonds, in benzene there is, in addition, the loss of extra stability associated with the delocalized wave functions of an aromatic system. The result is that benzene in the 1,2 configuration is more weakly bound than ethylene. The 1,4 configuration forms a stronger bond than the 1,2 configuration because it fits the geometry imposed by the (ideally) outward-pointing silicon dangling bonds. Note that the benzene 1,4 structure is closely related to the structure proposed for 1,3-cyclohexadiene adsorbed on Si(100). Because 1,3-cyclohexadiene is not aromatic, the net bonding strength is greater, at 2.3 eV.

Turning to the bridging structures, we found that the symmetric bridging configuration, Figure 4(*d*), was weakly bound, 0.20 eV (64). Although this structure fits the substrate well, the creation of a radical center on each of the two central carbon atoms is very unfavorable. The ground state structure (Figure 4*e*) referred to as the tight bridge is a less-symmetric bridging geometry with a calculated adsorption energy of 1.12 eV. This compares favorably with the barrier to desorption of 1.23 eV estimated from thermal desorption data (67). In the tight bridge configuration, four sequential carbon atoms rehybridize to sp^3 and bond to silicon, leaving a double bond between the remaining two carbon atoms. As the term "tight bridge" implies, the misfit between the molecule and the substrate is substantial. The Si dimers make a combined lateral move of 0.4 Å (64).

It is notable that the Ganz group was able to extract a lower bound on the energy difference between the one-dimer and the ground states of 0.14 eV (see Borovsky et al, 60). The energy difference between the calculated adsorption energies for the 1,4 and the tight bridge states is 0.08 eV (1.12–1.04) (64).

It emerges that the second observed bridge structure exists exclusively at type C defects that are always found on Si(100) at the level of ~1%. These appear as two parallel buckled dimers and are, I suspect, related to a subsurface structural

anomaly. As shown in Figure 4*f*, the twisted bridge structure, like the tight bridge, bonds through four sequential carbon atoms. In the twisted bridge, though, the structure is rotated, leaving the C-double bond at a right angle to the dimers. The calculated adsorption energy is 0.91 eV. This should be considered as only a rough guide because it is modeled on two regular dimers, not on a C defect. This result predicts that a clean dimer twisted bridge can exist but that it is metastable with respect to the 1,4 species or the tight bridge. Existing STM experiments permit only a lower bound of 1 eV to be estimated for the adsorption energy of the C defect twisted bridge species. A secondary desorption feature at 1.34 eV, attributed originally to adsorption at defects (67), may be due to the C defect twisted species.

Further support for the 1,4 and tight bridge structures comes from comparison of IR spectroscopic measurements and calculated spectra (63). Spectra recorded soon after benzene exposure were consistent with the 1,4 structure. Like the STM images, the spectrum evolved to include components related to the tight bridge structure.

To further discriminate between the candidate structures, STM images were simulated for each (64). The simulated images were obtained from constant electron density contours based on the highest occupied molecular orbitals. Within the Tersoff-Hamann approximation (24), these electron density contours correspond to a constant current STM image. Charge density iso-surfaces of occupied valence states were calculated for each of the bonding geometries (Figures 4*b–f*) and are shown as Figures 4*g–k*. It is important to note that contours calculated at the relatively modest HF/3-21G level after AM-1 optimization are very similar to those generated by rigorous calculations. The relatively inexpensive AM-1/HF/3-21G approach makes treatment of relatively large 4-dimer (27 Si-atom) clusters practical. The larger cluster, in turn, better facilitates comparison of real and simulated images. For the bright protrusions labeled *S* in Figure 4*a*, there are two possible candidate structures. The iso-surface for the 1,2 geometry (Figure 4*g*), predicts a maximum between the attached and an adjacent dimer, which is inconsistent with STM images. In contrast, the iso-surface for the 1,4 configuration (Figure 4*h*) shows two lobes, symmetrically placed above the reacted dimer, that are due to the double bonds formed on rehybridization of the molecule. It was concluded that the type *S* features in the image are due to the 1,4 structure shown in Figure 4*c*.

Each of the bridged structures has a distinctive charge density contour. The charge density iso-surface for the tight bridge structure (Figure 4*i*) predicts a maximum above one of the two affected dimers, whereas the twisted bridge geometry (Figure 4*j*) gives rise to a very similar feature, but rotated by 90°. The symmetric bridge (Figure 4*k*) exhibits two bright features symmetrically positioned between two dimers, arising from the two radical-like carbons. This contour does not correspond to any of the observed features in Figure 4*a*. Along with energetic considerations, this rules out the symmetric bridge structure. The features labeled *B1* and *B2* correspond well with the simulated images for the tight- and twisted

bridge geometries, respectively. For both of these configurations, the bright features are seen to correspond to the single remaining double bond on the bonded benzene molecule. The assignments based on simulated images, on adsorption energies, and on IR spectra are all in agreement.

It may seem that this system has been over-analyzed. STM structural and energy information, experimental and computed IR, computed structures, computed and experimental adsorption energies, and synthesized images have been considered. It was necessary to establish the nature of the benzene system securely to create a foundation upon which to build. Note that some of the analyses are not well established (cluster-based adsorption modeling is well known, yet still disfavored by some; image synthesis as described here is new) so the consistency of results lends credence to each of the various approaches. Furthermore, the structures identified are strange—we have no basis from which to draw to predict structures such as the tight bridge—and therefore these structures needed extra substantiation. Finally, the principles found for this prototype system will allow resolution of other problems without the full battery of techniques.

It is interesting to revisit 1,3-cyclohexadiene at this point. Possibly, the structure labeled *Z* in Figure 3*a* is analogous to the benzene tight bridge structure formed as the single-dimer-bound Diels-Alder product tips over to expend its remaining double bond to form two new C-Si bonds. We can further predict that type *X* features (the Diels-Alder product) will convert in time to type *Z* structures. Finally, the structure labeled type *Y* is possibly analogous to the twisted bridge species identified for adsorbed benzene. The alternate assignments, that *Y* and *Z* are di-σ structures, is at odds with the published calculations that found that the di-σ species face no barrier to conversion to the Diels-Alder product.

Carene Looking well into the future, we can imagine organically modified Si surfaces serving as sensors capable of complex molecular recognition tasks such as the ability to discriminate between different enantiomers of the same compound. Development in this area will require the design of enantiospecific reactions with the silicon surface. Lopinski et al (67a) provided the first example of such a reaction by demonstrating that the adsorption of 1*S*(+)-3-carene on the Si(100) surface is enantiospecific, resulting in the formation of four chiral centers and a chiral surface.

In the study of *cis*- and *trans*-2-butene, it was shown that reaction at both the *Re* and *Si* faces of the molecules was equally likely so that equal numbers of the two possible enantiomers were formed, resulting in a macroscopically achiral surface (49). In an effort to achieve enantioselective adsorption, 1*S*(+)-3-carene, a naturally occurring bicyclic alkene belonging to the terpene family, was chosen because in that molecule one face is blocked.

Optimized structures and adsorption energies of the configurations of Figure 5*a–c* were obtained using gradient-corrected density functional methods (B3P86 with the 6-31G* basis set). All three configurations exhibit substantial adsorption energies: The unbridged structures have similar adsorption energies,

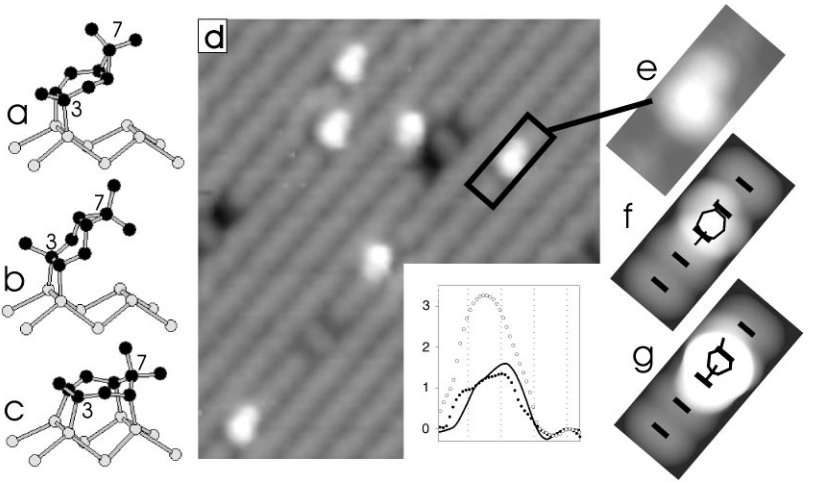

Figure 5 (*a–c*) Carene adsorption structures. In the text these are referred to as (*a*) unbridged, (*b*) reverse unbridged, and (*c*) bridge. (*d*) STM image (100 + Å^2, −2 V, 100 pA) of carene molecules adsorbed on Si(100). (*e*) Enlarged view of a single adsorbed carene molecule. (*f*) Simulated image for the bridging geometry of (*c*). (*g*) Simulated image for the unbridged geometry of (*a*). The *gray scale* in the two simulated images is the same. The saturation (to white) of the unbridged simulated image reflects the much higher maximum predicted for that structure—a prediction at odds with experiment.

2.25 eV (5*a*) and 2.07 eV (5*b*), whereas the bridged configuration is predicted to be substantially more stable, at 3.96 eV.

Figure 5*d* shows an STM image of the Si(100) surface after exposure to a low dose of 1*S*(+)-3-carene molecules. The protrusions all have a characteristic appearance consisting of a bright round maximum with a smaller tail asymmetrically positioned off to one side. Four of the molecules are of the same orientation, whereas the other two exhibit the same features but are rotated by 180°. The observation of these two different orientations assures that the tail is not a tip-shape artifact. By comparison with the calculated geometries in Figure 5*a–c*, the larger protrusion can be assigned as being primarily due to the two methyl groups at the C7 position of the adsorbed molecule, whereas the smaller protrusion is due to the C3 methyl group. Whereas two orientations of the molecule are observed in the image, these are identical structures related by a rotation, and hence they have the same chirality. Inspection of several hundred molecules indicated that reaction at one face of the molecule is indeed blocked, confirming that the reaction is enantiospecific.

In an attempt to distinguish between the bridged and unbridged bonding configurations, the observed molecular features were compared with simulated images for these two geometries. The simulated images were computed as for benzene.

Whereas both of the simulated images exhibit the correct chirality, the calculated image for the bridged geometry, Figure 5*g*, is seen to give better agreement with the observed features. In the simulated image for the unbridged configuration (Figure 5*d*), the C3-methyl protrusion that gives the image its asymmetric appearance is relatively less distinct and the image is dominated by the protrusion, which is due to the two C7-methyl groups. The largest distinction between the two simulated images is in the predicted maximum height with respect to a clean dimer: 1.3 Å and 3.3 Å for the bridged and unbridged configurations, respectively. The average maximum height of the molecules measured in the STM images varies somewhat with bias voltage, 1.7 Å at −2 V and 1.4 Å at −1.5 V. The good agreement between the measured and calculated heights suggests that the molecule adopts the bridging geometry.

If the molecule adopts the bridging configuration, it is possible that the unbridged configuration is a metastable precursor to the more stable geometry and is isolable at low temperature. Unlike the case of benzene-Si(100), where a slow conversion from a single dimer to bridging geometry was observed at room temperature (60, 62), no time-dependent change in the adsorbate bonding geometry was observed for carene. Adsorption into the bridge state at room temperature would imply that the barrier for opening the cyclopropyl ring and forming two additional Si-C bonds is less than 0.85 eV. The breaking of the cyclopropyl ring is somewhat surprising, as cyclopropane has been reported to not react with the Si(100) surface (68). Evidently, favorable positioning of the single-dimer–bound species together with the opportunity to make repeated attempts at cyclopropyl-dimer reaction leads to ring opening in the case of carene. We speculate that similar ring-opening reactions may serve to anchor various other organic molecules on Si(100). This bonding configuration is predicted to be highly stable, which suggests that carene-saturated Si(100) surfaces may be tolerant of air exposure.

Benzoic Acid and Aniline Benzoic acid (C_6H_5-COOH) and aniline (C_6H_5-NH_2) adsorption on Si(100) have been studied by EELS spectroscopy (vibrational spectroscopy) and LEED (69). For both molecules it was determined that deprotonation occurs to form one surface Si-H species per molecule. The benzoic acid and aniline molecules bond through Si-O-C and Si-N-C linkages, respectively. It was pointed out that these unidentate configurations are analogous to those exhibited by formic acid (HCOOH) and ammonia (NH_3) on Si(100).

It is notable that no C-H stretching at or below 3000 cm^{-1} was observed, as would be expected if the ring interacted with the surface directly (like benzene), creating sp^3 carbon atoms.

Considerable insight into the thermal stability of these molecules was also found. Upon annealing to 570K, the benzoic acid adsorbate decomposed, with benzene desorbing and CO_2 remaining on the surface. Aniline was found to be more resilient. On heating to 730K, some decomposition occurred, but intact molecules were still evident.

It is striking that these molecules with two or more modes of adsorption available—the Si-O-C/Si-N-C linkage as well as benzene-like direct ring interactions—show only the former. No rigorous, calculated adsorption energies are available, but we note that AM-1 calculations for benzoic acid show the Si-O-C linked configuration to be more stable than the direct ring-bonded modes, at 1.4 compared with 1.0 eV. It is interesting to speculate briefly on the adsorption dynamics. As randomly oriented molecules reach the surface, either they tumble and migrate in a physisorbed precursor state to find the Si-O-C/Si-N-C linkage (nearly) exclusively or the molecules find various chemisorbed positions, then subsequently convert to the upright state. It will be interesting to study this adsorption system with STM to see whether some fraction of the molecules do in fact acquire the flat benzene-like structure. Alternately, with EELS or STM, adsorption slightly below room temperature may show some benzene-like adsorption.

Phthalocyanine Convincing images of copper-phthalocyanine on Si(100) have been reported (70). This large, flat fourfold symmetric molecule is of classic interest in microscopy because it was the subject of the first single-molecule image using field emission microscopy (71). In the STM images, three distinct adsorption states are seen. In two of these, one of the long axes of this cross-like molecule lies directly over a dimer row, whereas the two other arms reach over to adjacent rows. The difference between these species is signaled by very different relative intensities in the images. Presumably, the two species are in different points of registry with the substrate and therefore have different electronic structures. The details of the bonding are unknown but could possibly be worked out if lattice-resolved images were available to extract exact registry. The third species observed is rotated to span only two dimer rows.

Copper-phthalocyanine and related molecules might serve as useful platforms or anchors for more complex molecular structures. It might be interesting to see whether by tailoring the molecule it could be induced to take only one position. A related, and larger, porphyrin molecule adsorbed on Au(110), Cu(100), and Ag(110) has also been examined with STM (72).

Wet Chemistry for the Organic Modification of Silicon

Historically, studies aimed at a microscopic understanding of adsorbate/surface structure have been limited to systems where the adsorbate was placed on the surface by gaseous deposition in ultra-high vacuum conditions. Of course, the semiconductor industry primarily uses vacuum deposition techniques to build up the complex structures that become microelectronic devices. Wet-chemical processing is essential for wafer cleaning and in some stages of lithography, but it is restricted to those uses.

As we search for methods for building and characterizing highly controlled molecule-surface structures, it seems appropriate that we go beyond the conventional

approach of placing adsorbates by use of dry methods, to consider the vast possibilities presented by wet-chemical methods. Furthermore, it is worth noting that some molecules, particularly biological molecules, cannot be vacuum-deposited because of lack of vapor pressure or because they will become denatured on removal from solution. Of course, if in the future one aims to make sensors of molecules in solution, it is essential that structures tolerant of that environment be developed. So in addition to using wet processing for building structures, we must begin to do more analysis in solution and in vacuum after solution exposure.

Although the emphasis in this review is on the Si(100) surface, the following descriptions of exclusively Si(111)-surface chemistry are included because that is all that exists at this time. Most research now uses as a starting point nearly perfect H-terminated Si(111) that can be easily created in a beaker (73). Although Si(100) can be similarly terminated, the surface ends up significantly roughened. It is hoped that new developments will emerge to allow translation of Si(111)-based knowledge to the more technologically relevant Si(100) surface. [The advantage Si(100) has over Si(111) is a more desirable Si/SiO_2 interface.] Although it seems unlikely at this point, it may be that Si(111)-based technology will emerge, perhaps driven by new processing possibilities. There is also a hybrid possibility involving V-shaped [111] trenches or ridges within otherwise [100]-based devices.

The work in solution-based modification of silicon is developing rapidly. Here, only key early work and a few samples of recent results are described.

In their pioneering work, Linford et al (74, 75) used free radical initiation to form close-packed alkyl monolayers on the Si(111) surface by reaction with H-Si(111). Initially, Linford et al (75) used thermal decomposition of diacyl peroxides $\{[CH_3(CH_2)_nC(O)O]_2, n = 16 \text{ and } 10\}$ to create alkyl radicals. They hypothesized that a radical could strip an H-atom from the surface, creating the opportunity for that surface silicon radical to combine with another alkyl radical to form an Si-R bond. Careful analysis with IR, X-ray photoelectron spectroscopy, surface wetting, and ellipsometry showed that densely packed films of alkyl groups directly linked through a Si-C bond were formed.

In a subsequent study, new possibilities were opened when it was shown that high-quality films could be produced by reacting 1-alkenes with H-Si(111) (75). A diacyl peroxide served as a free-radical initiator but was not significantly incorporated into the film. Using this approach, alkynes were also shown to form monolayers. X-ray reflectivity showed that the film density was ~90% of that for crystalline hydrocarbons. IR showed the films were densely packed, and IR dichroism revealed that the films were tilted from the normal and twisted about their axes. Wetting properties indicated that the films were methyl-terminated. The alkyl-Si(111) films were shown to be quite robust. Many weeks of air exposure caused little oxidation. A clean Si surface oxidizes instantly. It is remarkable that a film approximately 2 nm thick largely prevents oxidation. The monolayers were also shown to stand up to boiling chloroform, boiling water, boiling acidic and basic solutions, and fluoride.

In this same study (75), a mechanism is proposed that builds on the free-radical processes described by Linford & Chidsey (74). The same mechanism is invoked to create a surface-dangling bond (that is, a surface Si radical). It is suggested that an alkene subsequently reacts with that dangling bond to form a new Si-C bond and an alkyl radical. The alkyl radical in turn abstracts a hydrogen atom from an adjacent surface site, thereby setting up a chain reaction.

Bansal et al formed Si(111)-C linkages in a two-step process by first chlorinating the Si(111)-H surfaces and then reacting the Si(111)-Cl surface with alkyl-Grignard or alkyl-lithium reagents (76–78). A variety of surface-science techniques were used to monitor the process. X-ray photoelectron spectroscopy showed a Si 2p peak shifted to higher binding energy in accord with the formation of Si-Cl bonds in the first step of the process. EELS vibrational spectroscopy showed a peak at 560 cm^{-1}, consistent with surface Si-Cl. On reaction with alkyl-Grignard or alkyl-lithium reagents only Si, O, and C were detectable in X-ray photoelectronic spectroscopy. Vibrational spectroscopy was consistent with Si-C bonded alkyl-functionalized silicon. Although these initial films showed passivating behavior, significant Si oxidation occurred in air with a timescale of several hours.

A halogenation/thienylation route has been used to form thiophene derivitized Si(111) (79). Boukherroub et al have shown that surfaces similar to those obtained by the two-step halogenation/alkylation process could be obtained in a direct thermal reaction of alkylmagnesium bromides with H-Si(111) (80).

The photochemical hydrosilylation of aldehydes in a reaction with H-Si(111) to form silicon alkoxy bonds (Si-O-R)-surfaces was recently demonstrated (81). Two thermal routes to the formation of Si-O-R on Si(111) have now been described (81a). In that work it was noted that there appear to be a number of parallels between silicon surface chemistry and organosilicon molecular chemistry. No doubt many creative routes to variously functionalized silicon surfaces await discovery.

ADSORPTION DYNAMICS AND COUPLING

In these early days of learning to make well-defined adsorbed organic structures, most work is directed at structural determination. Likely, issues related to adsorption dynamics and coupling of adsorbates will also need to be wrestled with before we have a foundation laid for building complex molecular devices. The work done so far in this area suggests that many interesting phenomena await our inspection. Perhaps we should not view studies of these other issues as detours but rather as opportunities to discover new principles.

Space restrictions prevent a thorough discussion of this area. As a compromise, a few examples are mentioned to suggest some of the factors acting to affect, and possibly to limit, the control with which small molecular structures can be built.

The recognition that adsorbates couple or in some way to affect one another's position or energy is as old as surface science. Since STM became available, many

interesting microscopic details of adsorbate interactions have become visible. Often, these have not been the central object of interest. The bar-like trenches that seem inevitably to form on Si(100) and that seem to be related to Ni contaminants are one example of adsorbate clustering. These and other contaminant-related structures grow not randomly, but with some degree of registry with the substrate. In a study of water adsorption on Si(100), Chander et al showed that water molecules formed clusters and chains (82). Another microscopic view of adsorbate interactions (83) showed that chains of adsorbed CO formed on Cu(110) and that single adsorbates within the chain made small jumps with more ease than isolated adsorbates did.

Particularly graphic examples of through-substrate adsorbate interactions were seen in the study of Si-atom adsorption on Si(100) (84). In that study, atoms were seen to behave as coupled even though positioned in adjacent rows, or even one or two rows removed. The paired atoms were observed to move, but that motion was restricted to a line at right angles to the dimer rows. It is important to note that the barrier controlling that motion was smaller than that experienced by an isolated atom. There was direct evidence that the atoms altered their immediate surroundings through a strain field. The dimer buckling pattern in a row intervening between paired atoms was seen to have a disruption, as if an adsorbate was placed there.

The silicon atom on Si(100) experiment also provided rare evidence of another adsorption phenomenon that may be important in efforts to position molecules precisely. This effect, sometimes called transient mobility, is related to the disposal of energy, specifically of the heat of adsorption that is instantaneously available when the adsorbate forms a surface bond. Initially held as local internal energy, this heat very quickly leaks into the system to leave the adsorbate in equilibrium with the substrate. Before the cooling occurs, on a timescale of a few vibrational periods, the adsorbate is hot and can possibly migrate on the surface. (For Si-atoms, the heat of adsorption is on the order of several electron volts, whereas the barrier to diffusion is about 0.6 eV.) The nonrandom distribution of Si-atoms seen in (84) required that the atoms take several steps before coming to rest, indicating that transient mobility played a role. Similar effects are anticipated when a large heat of adsorption and a small barrier to diffusion exist.

The coupling mechanisms that allow energy to be dissipated are complex and system dependent. The challenge to theory in this area is formidable. However, progress is being made. [For a recent example of work in this area and for related references see Kindt et al (85).] There, CO on Cu(100) was studied to assess the contributions of electron-hole pair excitations in sticking, scattering, and diffusion.

Another, and much more general, mode of adsorbate mobility is ascribed to the existence of precursors to chemisorption. These are short-lived physisorbed species that allow the molecule to tumble and migrate to select an adsorption site. Careful kinetic measurements were used to implicate a precursor mediated-adsorption process in the case of ethylene on Si(100) (35). With STM, each time an adsorbate shows a preference for one site over another nonequivalent type of

site, a precursor is implicated. We see that molecules do not necessarily stick at their point of impact. The first example of this was the ammonia Si(111)-(7 × 7) study where site type-specific adsorption statistics were noted (22). Despite many indirect indications of physisorbed precursors, there remained some doubt about the existence of these species. Recently, Brown et al succeeded in capturing and imaging benzene molecules in the precursor state on Si(111)-(7 × 7) (86). Kinetics for the decay to the chemisorbed state were recorded and the precursor state lifetime was shown to vary with temperature. Likely, all the molecules reviewed here pass through a similar precursor state.

As a final note in this section, I wish to point out that regular thermally activated molecular diffusion on a silicon surface is highly restricted. Very few studies have probed this area. In the only STM study, it was shown that benzene molecules were as likely to desorb as to diffuse on Si(111)-(7 × 7) (87). Unlike metal atoms on metal surfaces where very small barriers to diffusion exist, molecules on silicon cannot readily begin to form bonds to a new site smoothly and in compensation for bonds breaking at a present site. This inability to "make before break" leads to large barriers. Work in progress (87a) shows that the benzene Si(111)-(7 × 7) case was not an anomaly. This frustrated diffusion will place limitations on future schemes for creating molecular structures on silicon.

TOOLS FOR MAKING PROTOTYPE STRUCTURES

When Eigler & Schweitzer controllably moved Xe-atoms with an STM, they captured the imagination of scientists and lay people alike (88). This enormous advance showed that STM could be used not only to image but to manipulate at the atomic scale. Many exciting advances have since been made, unfortunately too many to review here. The controlled breaking of Si-H-bonds is particularly interesting in the current context. Different bond-breaking modes have been identified and are summarized by Avouris et al (89). Controlled H-removal is interesting because it allows atomic-scale patterning on an H-terminated Si(100) surface. The silicon dangling bonds made available can be used as reactive sites in a subsequent step. Because H-terminated regions are passive to many reactants, spatially controlled growth of structures can, in principle, be achieved. Fine Al lines have been formed in this manner (90).

Even though STM-based patterning may never be a viable commercial process, it is likely that characterization of small structures created through this route will be important stepping-stones to new nano-scale device concepts. The first steps in this direction have been made. Studies, both experimental (91) and theoretical (92), have recently aimed to understand lines of dangling bonds created with STM on an H-terminated Si surface. We may anticipate similar studies involving lines and arrays of adsorbates in the near future.

As a final note, I wish to mention one particularly interesting nano-scale pattern-forming process (93). Very thin (3 Å) and uniform SiO_2 films were electron

beam-irradiated to create very small and well-defined SiO regions. When annealed, SiO is volatilized, leaving patches of clean silicon several hundred Angstroms across, surrounded by SiO_2. In a study by Shibata et al, three small pads separated by approximately 100 nm are shown (93). Combined with other ideas mentioned in this review, this process may provide a route to rudimentary devices for measuring transport properties of hybrid adsorbate-Si systems.

THE FUTURE

In this review I have attempted to describe all organic adsorbate-Si(100) systems that have been studied. Many different bonding interactions remain to be explored. Various experimental methods have been and will continue to be used. Without question, STM is the key enabling tool and the technique that will move us closer to properties that can be harnessed and to new device concepts. STM makes available the electronic signature, the placement, and the spatial symmetry of an adsorbate. At times this allows for an educated guess at the structure; for more complex adsorbates, detailed structural assignment based on STM features alone is not be possible. It is essential then to use some form of theoretical modeling to understand STM images better. Calculations, both ab initio and inexpensive AM-1 types, are now indispensible and highly accessible tools. In many cases, the experimentalist can, and must, do in-house calculations to progress efficiently. The availability of excellent commercial software and powerful inexpensive computers makes this an entirely practical thing to do. In addition to calculated adsorption energies, structures, and vibrational spectra, it has been shown here that a simple new method for STM-image simulation is a powerful discriminator of candidate structures.

As exciting and challenging as structural determinations are, we must not lose sight of the need for understanding adsorption dynamical issues. It may well emerge that key new principles, specific to the microscopic realm, will be the properties that enable and make worthwhile truly molecular-scale devices.

STM and ultra-fine electron beam-based methods for fabrication seem tantalizingly close to allowing construction of structures for transport characterization and testing of simple device concepts.

LITERATURE CITED

1. Whitesides GM. 1995. *Sci. Am.* 273(3): 146–49
2. Camillone N, Eisenberger P, Leung TYB, Schwartz P, Scoles G, et al. 1994. *J. Chem. Phys.* 101:11031–36
3. Brown AR, Pomp A, Hart CM, de Leeuw DM. 1995. *Science* 270:972–74
4. Crooks RM, Ricco AJ. 1998. *Acc. Chem. Res.* 31:219–27
5. Gimzewski JK, Jung TA, Cuberes MT, Schlittler RR. 1997. *Surf. Sci.* 386:101–14
6. Bradshaw AM. 1997. *Curr. Opin. Solid State Mater. Sci.* 2:530–38
7. Brus LE, Szajowski PF, Wilson WL,

Harris TD, Schuppler S, Citrin PH. 1995. *J. Am. Chem. Soc.* 117:2915–22
8. Luedtke WD, Landman U. 1994. *Phys. Rev. Lett.* 73:569–72
9. First PN, Stroscio JA, Dragoset RA, Pierce DT, Celotta RJ. 1989. *Phys. Rev. Lett.* 63:1416–19
10. McComb DW, Collings BA, Wolkow RA, Moffatt DJ, MacPherson CD, et al. 1996. *Chem. Phys. Lett.* 251:8–12
11. Huang L, Chey SJ, Weaver JH. 1998. *Phys. Rev. Lett.* 80:4095–98
12. Carter FL. 1983. *J. Vac. Sci. Technol. B* 1: 959–68
13. Binnig G, Rohrer H, Gerber Ch, Weibel E. 1982. *Phys. Rev. Lett.* 49:57–60
14. Schlier RE, Farnsworth HE. 1959. *J. Chem. Phys.* 30:917–22
15. Hamers RJ, Tromp RM, Demuth JE. 1986. *Phys. Rev. B* 34:5343–49
16. Wolkow RA. 1992. *Rev. Sci. Instrum.* 63: 4049–53
17. Wolkow RA. 1992. *Phys. Rev. Lett.* 68: 2636–39
18. Schluter M. 1988. *The Chemical Physics of Solid Surfaces and Heterogeneous Catalysis*, ed. DA King, DP Woodruff, 5:37–68. Amsterdam: Elsevier
19. Duke CB. 1996. *Chem. Rev.* 96:1237–59
20. Becker R, Wolkow RA. 1993. In *Scanning Tunneling Microscopy, Methods of Experimental Physics Ser.*, ed. J Stroscio, W Kaiser. New York: Academic
21. Kubby JA, Boland JJ. 1996. *Surf. Sci. Rep.* 26:62–96
22. Wolkow RA, Avouris Ph. 1988. *Phys. Rev. Lett.* 60:1049–52
23. Avouris Ph, Wolkow RA. 1989. *Phys. Rev. B* 39:5091–99
24. Tersoff J, Hamann DR. 1985. *Phys. Rev. B* 31:805–13
25. Lang ND. 1985. *Phys. Rev. Lett.* 55:230–33
26. Lang ND. 1986. *Phys. Rev. Lett.* 58:45–48
27. Eigler DM, Weiss PS, Schweizer EK, Lang ND. 1991. *Phys. Rev. Lett.* 66:1189–92
28. Hallmark VM, Chiang S, Meinhardt KP, Hafner K. 1993. *Phys. Rev. Lett.* 70:3740–43
29. Sautet P, Joachim C. 1991. *Chem. Phys. Lett.* 185:23–27
30. Sautet P, Joachim C. 1992. *Surf. Sci.* 271: 387–95
31. Bocquet ML, Sautet P. 1996. *Surf. Sci.* 360:128–36
32. Sautet P, Bocquet ML. 1996. *Phys. Rev. B* 53:4910–25
33. Bozack MJ, Taylor PA, Choyke WJ, Yates JT. 1986. *Surf. Sci.* 177:933–37
34. Yoshinobu J, Tsuda H, Onchi M, Nishijima M. 1987. *J. Chem. Phys.* 87:7332–40
35. Clemen L, Wallace RM, Taylor PA, Dresser MJ, Choyke WJ, et al. 1992. *Surf. Sci.* 268:205–16
36. Pan W, Zhu T, Yang W. 1997. *J. Chem. Phys.* 107:3981–85
37. Fisher AJ, Blochl PE, Briggs GAD. 1997. *Surf. Sci.* 374:298–305
38. Mayne AJ, Avery AR, Knall J, Jones TS, Briggs GAD, Weinberg WH. 1993. *Surf. Sci.* 284:247–56
39. Ness H, Fisher AJ, Briggs GAD. 1997. *Surf. Sci.* 380:L479–84
40. Ness H, Fisher AJ. 1997. *Phys. Rev. B* 55:1–13
41. Nishijima M, Yoshinobu J, Tsuda H, Onchi M. 1987. *Surf. Sci.* 192:383–97
42. Taylor PA, Wallace RM, Cheng CC, Weinberg WH, Dresser MJ, et al. 1992. *J. Am. Chem. Soc.* 114:6754–60
43. Liu Q, Hoffmann R. 1995. *J. Am. Chem. Soc.* 117:4082–92
44. Imamura Y, Morikawa Y, Yamasaki T, Nakatsuji H. 1995. *Surf. Sci.* 341:L1091–96
45. Meng B, Maroudas D, Weinberg WH. 1997. *Chem. Phys. Lett.* 278:97–101
46. Huang C, Widdra W, Wang XS, Weinberg WH. 1993. *J. Vac. Sci. Technol. A* 11:2250–54
47. Li L, Tindall C, Takaoka O, Hasegawa Y, Sakurai T. 1997. *Phys. Rev. B* 56:4648–55
48. Carner CS, Weiner B, Frenklach M. 1993. *J. Chem. Phys.* 99:1356–72

48a. Wolkow RA. Unpublished results
49. Lopinski GP, Moffatt DJ, Wayner DDM, Wolkow RA. 1998. *Nature* 392:909–12
50. Kiskinova M, Yates JT. 1995. *Surf. Sci.* 325:1–10
51. Fang H, Giancarlo LC, Flynn GW. 1998. *J. Phys. Chem. B* 102:7311–15
52. Hamers RJ, Hovis JS, Lee S, Liu HB, Shan J. 1997. *J. Phys. Chem.* 101:1489–92
53. Padowitz DF, Hamers RJ. 1998. *J. Phys. Chem. B* 102:8541–45
54. Hovis JS, Hamers RJ. 1997. *J. Phys. Chem. B* 101:9581–85
55. Konecny R, Doren DJ. 1997. *J. Am. Chem. Soc.* 119:11098–99
56. Teplyakov AV, Kong MJ, Bent SF. 1997. *J. Am. Chem. Soc.* 119:11100–1
57. Hovis JS, Liu H, Hamers RJ. 1997. *Surf. Sci.* 402:1–7
58. Hovis JS, Hamers RJ. 1998. *J. Phys. Chem. B* 102:687–92
59. Kasaya M, Tabata H, Kawai T. 1998. *Surf. Sci.* 400:367–74
60. Borovsky B, Krueger M, Ganz E. 1998. *Phys. Rev. B* 57:4269–72
61. Joeng HD, Ryu S, Lee YS, Kim S. 1995. *Surf. Sci.* 344:L1226–29
62. Lopinski GP, Fortier TM, Moffatt DJ, Wolkow RA. 1998. *J. Vac. Sci. Technol. A* 16:1037–42
63. Lopinski GP, Moffatt DJ, Wolkow RA. 1998. *Chem. Phys. Lett.* 282:305–12
64. Wolkow RA, Lopinski GP, Moffatt DJ. 1998. *Surf. Sci.* 416:L1107–12
65. Gokhale S, Trischberger P, Menzel D, Widdra W, Droge H, et al. 1998. *J. Chem. Phys.* 108:5554–64
66. Birkenheuer U, Gutdeutsch U, Rosch N. 1998. *Surf. Sci.* 409:213–28
67. Taguchi Y, Fujisawa M, Takaoka T, Okada T, Nishijima M. 1991. *J. Chem. Phys.* 95:6870–78
67a. Lopinski GP, Moffatt DJ, Wayner DDM, Wolkow RA. 1999. *J. Am. Chem. Soc.* 121:4532–35
68. Yates JT. 1991. *J. Phys. Condens. Matter* 3:S143–56
69. Bitzer T, Alkunshalie T, Richardson NV. 1996. *Surf. Sci.* 368:202–7
70. Kanai M, Kawai T, Motai K, Wang XD, Hashizume T, Sakura T. 1995. *Surf. Sci.* 329:L619–23
71. Melmud AJ, Muller EW. 1958. *J. Chem. Phys.* 29:1037–45
72. Jung TA, Schlittler RR, Gimzewski JK. 1997. *Nature* 386:696–98
73. Higashi GS, Chabal YJ, Trucks GW, Raghavachari K. 1990. *Appl. Phys. Lett.* 12:656–58
74. Linford MR, Chidsey CED. 1993. *J. Am. Chem. Soc.* 115:12631–32
75. Linford MR, Fenter P, Eisenberger PM, Chidsey CED. 1995. *J. Am. Chem. Soc.* 117:3145–55
76. Bansal A, Li X, Lauerman I, Lewis NS. 1996. *J. Am. Chem. Soc.* 118:7225–26
77. Bansal A, Lewis NS. 1998. *J. Phys. Chem. B* 102:1067–70
78. Bansal A, Lewis NS. 1998. *J. Phys. Chem. B* 102:4058–60
79. He J, Patitsas SN, Preston KF, Wolkow RA, Wayner DDM. 1998. *Chem. Phys. Lett.* 286:508–14
80. Boukherroub R, Bensebaa F, Morin S, Wayner DDM. 1999. *Langmuir.* In press
81. Effenberger F, Gotz G, Bidlingmaier B, Wezstein M. 1998. *Agnew. Chem. Int. Ed. Engl.* 37:2462–64
81a. Boukherroub R, Morin S, Wayner DDM. 1999. *Langmuir.* Submitted for publication
82. Chander M, Li YZ, Patrin JC, Weaver JH. 1993. *Phys. Rev. B* 48:2493–99
83. Briner BG, Doering M, Rust HP, Bradshaw AM. 1997. *Science* 278:257–60
84. Wolkow RA. 1995. *Phys. Rev. Lett.* 74: 4448–51
85. Kindt JT, Tully JC, Head Gordon M, Gomez MA. 1998. *J. Chem. Phys.* 109: 3629–36

86. Brown DE, Moffatt DJ, Wolkow RA. 1998. *Science* 279:542–44
87. Wolkow RA, Moffatt DJ. 1995. *J. Chem. Phys.* 103:10696–700
87a. Patitsas SN, Lopinski GP, Wolkow RA. Submitted for publication
88. Eigler DM, Schweizer EK. 1990. *Nature* 344:524–26
89. Avouris Ph, Walkup RE, Rossi AR, Akpati HC, Nordlander P, et al. 1996. *Surf. Sci.* 363:368–77
90. Shen TC, Wang C, Tucker JR. 1997. *Phys. Rev. Lett.* 78:1271–74
91. Hitosugi T, Hashizume T, Heike S, Watanabe S, Wada Y, et al. 1997. *Jpn. J. Appl. Phys.* 36:L361–64
92. Watanabe S, Ono YA, Hashizume T, Wada Y, Yamauchi J, Tsukada M. 1995. *Phys. Rev. B* 52:10768–71
93. Shibata M, Nitta Y, Fujita K, Ichikawa M. 1998. *Appl. Phys. Lett.* 73:2179–81
93a. Wolkow RA. Unpublished results

Annual Review of Physical Chemistry
Volume 50, 1999

CONTENTS